ELSEVIER

NeuroImage

www.elsevier.com/locate/ynimg
NeuroImage 31 (2006) 496 – 504

# Changes in hippocampal connectivity in the early stages of Alzheimer's disease: Evidence from resting state fMRI

Liang Wang,[a] Yufeng Zang,[d] Yong He,[d] Meng Liang,[d] Xinqing Zhang,[b] Lixia Tian,[d] Tao Wu,[b,c] Tianzi Jiang,[d,*] and Kuncheng Li[a,*]

[a]*Department of Radiology, Xuanwu Hospital of Capital University of Medical Sciences, Beijing 100053, P.R. China*
[b]*Department of Neurology, Xuanwu Hospital of Capital University of Medical Sciences, Beijing 100053, P.R. China*
[c]*Beijing Institute of Geriatrics, Beijing 100053, P.R. China*
[d]*National Laboratory of Pattern Recognition, Institute of Automation, Chinese Academy of Sciences, Beijing 100080, P.R. China*

Received 10 July 2005; revised 14 December 2005; accepted 20 December 2005
Available online 9 February 2006

**A selective distribution of Alzheimer's disease (AD) pathological lesions in specific cortical layers isolates the hippocampus from the rest of the brain. However, functional connectivity between the hippocampus and other brain regions remains unclear in AD. Here, we employ a resting state functional MRI (fMRI) to examine changes in hippocampal connectivity comparing 13 patients with mild AD versus 13 healthy age-matched controls. Hippocampal connectivity was investigated by examination of the correlation between low frequency fMRI signal fluctuations in the hippocampus and those in all other brain regions. We found that functional connectivity between the right hippocampus and a set of regions was disrupted in AD; these regions are: medial prefrontal cortex (MPFC), ventral anterior cingulate cortex (vACC), right inferotemporal cortex, right cuneus extending into precuneus, left cuneus, right superior and middle temporal gyrus and posterior cingulate cortex (PCC). We also found increased functional connectivity between the left hippocampus and the right lateral prefrontal cortex in AD. In addition, rightward asymmetry of hippocampal connectivity observed in elderly controls was diminished in AD patients. The disrupted hippocampal connectivity to the MPFC, vACC and PCC provides further support for decreased activity in "default mode network" previously shown in AD. The decreased connectivity between the hippocampus and the visual cortices might indicate reduced integrity of hippocampus-related cortical networks in AD. Moreover, these findings suggest that resting-state fMRI might be an appropriate approach for studying pathophysiological changes in early AD.**


*Keywords:* Alzheimer's disease; Hippocampus; Functional MRI; Functional connectivity; Resting state

## Introduction

Alzheimer's disease (AD) is a progressive neurodegenerative disorder characterized by the presence of amyloid aggregations and neurofibrillary tangles (NFTs) together with a loss of cortical neurons and synapses (Terry, 1991; Nestor et al., 2004). NFTs selectively afflict specific cortical layers in the hippocampal formation (Hirano and Zimmerman, 1962). These cortical layers serve as the gateway of neural projection between hippocampal formation and the rest of the brain (de Lacoste and White, 1993). Therefore, cellular damage in these specific cortical layers may disconnect hippocampal formation from the cerebral cortex (Hyman et al., 1984, 1986) and raise the possibility that functional interactions between the hippocampus and other related brain regions may be abnormal in the early stages of AD (Delbeuck et al., 2003).

Functional neuroimaging is increasingly being used to study functional connectivity between distinct brain regions. Functional connectivity in imaging refers to a descriptive measure of spatio-temporal correlations between distinct regions of the cerebral cortex (Friston et al., 1993). By examining the correlation between regional cerebral blood flow (rCBF) in a referential region and all other brain voxels, Grady et al. (2001) described disrupted functional connectivity between the right prefrontal areas and the right hippocampus during face memory in AD using positron emission tomography (PET).

Functional connectivity can also be extracted from spontaneous activity of the resting brain. During the resting state, high temporal coherence of low-frequency (<0.08 Hz) fluctuations (LFFs) in fMRI time series has been observed between spatially distinct functionally related brain regions (Biswal et al., 1995, 1997a; Lowe et al., 1998). These LFFs in MR signal intensity are supposed to arise from fluctuations in capillary blood flow and blood oxygenation, which are, at least in part, secondary to neuronal activity (Biswal et al., 1995, 1997a,b). The synchrony of LFFs implies that there are underlying neural connections

* Corresponding authors. K. Li is to be contacted at Department of Radiology, Xuanwu Hospital of Capital University of Medical Sciences, Beijing 100053, P.R. China. Fax: +86 10 63013355x2376. T. Jiang, National Laboratory of Pattern Recognition, Institute of Automation, Chinese Academy of Sciences, Beijing 100080, P.R. China. Fax: +86 10 6255 1993.
*E-mail addresses:* jiangtz@nlpr.ia.ac.cn (T. Jiang), li_cums@yahoo.com.cn (K. Li).
**Available online on ScienceDirect (www.sciencedirect.com).**

1053-8119/$ - see front matter © 2005 Elsevier Inc. All rights reserved.
doi:10.1016/j.neuroimage.2005.12.033

(Lowe et al., 2000). Using this low frequency correlation approach, functional connectivity has been shown between motor (Biswal et al., 1995; Jiang et al., 2004), visual (Lowe et al., 1998), auditory (Cordes et al., 2001) cortices, language areas (Hampson et al., 2002), between the hippocampus and thalamus (Stein et al., 2000), and between the hippocampi (Rombouts et al., 2003).

Recently, Li et al. (2002) found that AD patients showed decreased synchrony of LFFs within the hippocampus. However, as stated above, AD involves a disconnection syndrome between dissociating neuronal systems (de Lacoste and White, 1993; Delbeuck et al., 2003). Thus, it is crucial to consider the interaction between distinct cerebral regions. Furthermore, Grady et al. (2001) described disrupted functional connectivity between the right prefrontal areas and the right hippocampus under task conditions. Therefore, we hypothesized that resting-state hippocampal connectivity, i.e., the correlation between LFFs in the hippocampus and those in all other brain regions, would be altered during the early stages of AD.

A primary method used to investigate functional connectivity for a specific region in fMRI is the "seed voxel" approach (Biswal et al., 1995). Given the existence of extensive afferent and efferent neocortical connections in the anterior hippocampus, this region seems situated to integrate neural activity from widespread neocortical inputs and outputs (Sperling et al., 2003). Therefore, we selected this region to examine alterations in hippocampal connectivity by means of a resting state fMRI.

## Materials and methods

### *Subjects*

Twenty-eight right-handed subjects participated in this study after giving written informed consent. This study was approved by the Medical Research Ethics Committee of Xuanwu Hospital. The 14 AD subjects were recruited from patients who consulted a memory clinic at Xuanwu Hospital for their memory complaints. The 14 healthy elderly controls were recruited by advertisements from the local community. The elderly control group and the AD group were matched by gender and age (within 2 years). For this purpose, all potential respondents for the advertisements were considered in the order received until a satisfactory gender and age-match with the AD patients was achieved. Table 1 contains descriptive demographic and neuropsychological data for the two groups. Data from two subjects (one AD patient and his corresponding age-matched control subject) were excluded from analyses due to this AD patient's excessive head motion during scanning (see Data Preprocessing).

All AD patients underwent a complete physical and neurological examination, standard laboratory tests and an extensive battery of neuropsychological assessment. The brain MRI scans for diagnostic evaluation showed no abnormality other than brain atrophy in the AD patients. The diagnosis of AD fulfilled the *Diagnostic and Statistical Manual of Mental Disorders, 4th Edition* (DSM-IV; American Psychiatric Association, 1994) criteria for dementia, and the National Institute of Neurological and Communicative Disorders and Stroke/Alzheimer Disease and Related Disorders Association (NINCDS-ADRDA) (McKhann et al., 1984) criteria for AD. Eight of 14 patients had a Clinical Dementia Rate (CDR) (Morris, 1993) score of 1, and were thus assigned to a mild AD category. The other six patients had a CDR score of 0.5. The cognitive impairment in these patients involved not only memory, but also several other CDR domains. Since a clinical progression and neuropathological study has indicated that such "CDR of 0.5" population represents early-stage AD (Morris et al., 2001), these six patients were considered to be in a very mild AD category.

Table 1
Demographics and clinical finding

| | AD ($n$ = 13) | Controls ($n$ = 13) | $P$ value |
|---|---|---|---|
| Sex, female/male | 8/5 | 8/5 | >0.99[a] |
| Age, year | 70.1 ± 6.7 | 69.5 ± 5.7 | 0.80* |
| Education, year | 8.9 ± 4.9 | 9.7 ± 4.2 | 0.68* |
| MMSE | 23.1 ± 3.1 | 28.9 ± 0.9 | <0.0001* |

MMSE, Mini-Mental State Examination; values are means ± SD.
[a] $P$ values were obtained using a Pearson $\chi^2$ two-tailed test, with continuity correction for $n < 5$.
* The $P$ value was obtained by a two-sample two-tailed $t$ test.

The criteria for healthy elderly were as follows: (1) no neurologic and psychiatric disorders, (2) no neurological deficiencies, (3) no abnormal finding in conventional brain MR imaging, (4) no cognitive complaints and (5) an MMSE score of 28 or higher.

### *Data acquisition*

All experiments were performed with a Siemens 1.5-T Magnetom Sonata system using a standard headcoil. Foam padding and headphones were used to limit head motion and reduce scanner noise. Structural images were acquired using a sagittal magnetization prepared rapid gradient echo (MP-RAGE) three-dimensional T1-weighted sequence (repetition time [TR] = 1970 ms, echo time [TE] = 3.9 ms, inversion time [TI] = 1100 ms, flip angle [FA] = 15°). For this resting-state fMRI, subjects were instructed to simply keep their eyes closed and to not think of anything in particular. Functional images were collected by using a gradient-echo echo-planar sequence sensitive to BOLD contrast (TR = 2000 ms, TE = 60 ms, FA = 90°). Whole-brain volumes were acquired with 20 contiguous 5-mm thick transverse slices, with a 2-mm gap and 3.75 × 3.75 mm in-plane resolution. At the same locations as the functional images, a T1-weighted sequence (TR = 500 ms, TE = 7.7 ms, FA = 90°) was acquired for anatomical information.

### *Data preprocessing*

Unless otherwise stated, all analyses were conducted using the AFNI package (Cox, 1996). The first 10 image acquisitions of the resting state were discarded because of spin saturation effects and adaptation of subjects to their immediate environment. The remaining 170 images were preprocessed, which included slice timing, motion correction, spatial normalization (Talairach and Tournoux, 1988) and resampling to 3 mm isotropic voxels followed by spatial smoothing with a 4 mm full width at half maximum (FWHM) Gaussian kernel. Following this, temporal filtering (0.01 Hz < $f$ < 0.08 Hz) was applied to the time series of each voxel to reduce the effect of low-frequency drifts and high-frequency noise (Greicius et al., 2003; Biswal et al., 1995; Lowe et al., 1998). One healthy

elderly subject lacked twenty-slice anatomical data, so the spm2 (http://www.fil.ion.ucl.ac.uk/spm) was used to coregister this subject's functional images to her own 3D anatomical images that were later transformed into stereotaxic coordinates space of Talairach (Talairach and Tournoux, 1988).

Each subject's movement parameters were examined. Datasets with more than 1.5 mm maximum translation in $x$, $y$ or $z$, or 1.5° of maximum rotation about three axes were discarded. Excessive movement was found in one AD (CDR = 1) subject's data using the above criteria. The data from this patient and the corresponding age-matched control subject were excluded from subsequent analyses. Since correlation analysis is very sensitive to gross head motion, we further characterized the head motion as an index representing the peak displacement that was determined by a method initiated by Jiang et al. (1995) and further used by Lowe et al. (1998). A two-tailed two-sample $t$ test was performed on the peak displacement to examine between-group differences in head motion.

In this study, twenty-slice T1 anatomical images did not cover the whole brain so that the most superior or inferior parts of the brain in some subjects were not scanned. Thus, a mask file was generated according to the intersection of 25/26 subjects' normalized T1 anatomical images (one subject had no anatomical images as was described above). Only the voxels within the mask were further processed.

### *Definition of region of interest (ROI)*

After spatial normalization, bilateral hippocampi were outlined manually on the coronal slice located at the dorsal margin of the mamillary body on high-resolution 3D images (Fig. 1). The hippocampal border was determined at this level as follows: dorsally and laterally, the alveus (white matter tract) provides a landmark; ventrally, the gray–white matter interface between the subiculum and the parahippocampal gyrus white matter is the boundary; medially, the hippocampus was demarcated by cerebrospinal fluid (CSF) in the transverse fissure and uncal sulcus; the amygdalohippocampal transition area was excluded from ROI (Duvernoy, 1998; Watson et al., 1992). The margin of these boundaries was not included in the ROI to avoid "contamination" from adjacent non-hippocampal tissue when the ROI was sampled down to the spatial resolution of fMRI images. All ROIs were drawn by a senior neuroradiologist (L.W.).

Finally, the subject-specific bilateral hippocampal ROIs were acquired from 26 subjects. Given the much lower spatial resolution of fMRI scans compared with the structural images, only voxels in fMRI images that were covered for more than 55% by the original structural ROI were used for further analyses. The rationale for this procedure has been presented in two previous studies (Li et al., 2002; Rombouts et al., 2003).

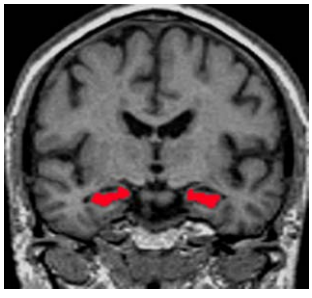

Fig. 1. Regions of interest (red) are manually drawn on the anterior hippocampus from a representative subject.

### *Functional connectivity analyses*

A seed reference time course was obtained by averaging the survived time courses within the ROI. Correlation analysis was carried out between the seed reference and the whole brain in a voxel-wise manner. A Fisher's $z$-transform was applied to improve the normality of these correlation coefficients (Press et al., 1992; Lowe et al., 1998). The individual $z$ value was entered into a random effect one-sample $t$ test in a voxel-wise manner to determine brain regions showing significant connectivity to the right and left hippocampi within each group. These values were also entered into a random effect two-sample $t$ test in a voxel-wise manner to identify the regions showing significant differences in connectivity to the right and left hippocampi between the groups (Holmes and Friston, 1998).

### *Group statistical maps*

Within experimental groups a single voxel threshold was set at $|t(12)| \geq 3.054$, $P < 0.01$ and a minimum cluster size of 513 $mm^3$ was used to correct for multiple comparisons. This yielded a corrected threshold of $P < 0.004$ in each group, determined by Monte Carlo simulation (see program AlphaSim by D. Ward in AFNI software. Parameters were: single voxel $P$ value = 0.01, FWHM = 4 mm, with mask. Also see http://afni.nimh.nih.gov/pub/dist/doc/manual/AlphaSim.pdf), to show significant connectivity to the right and left hippocampi.

Between experimental groups a single voxel threshold was set at $|t(24)| \geq 2.492$, $P < 0.02$ and a minimum cluster size of 513 $mm^3$ was used to correct for multiple comparisons. This yielded a corrected threshold of $P < 0.05$, determined by Monte Carlo simulation (see program AlphaSim by D. Ward in AFNI software. Parameters were: single voxel $P$ value = 0.02, FWHM = 4 mm, with mask. Also see http://afni.nimh.nih.gov/pub/dist/doc/manual/AlphaSim.pdf). This enabled the identification of changes in hippocampal connectivity in the AD group as compared with the healthy age-matched group.

Statistical parametric maps were overlaid on an average of the Talairach-normalized high-resolution 3D T1-weighted images from all subjects and the locations of regions showing significant connectivity to hippocampi were interpreted using known neuroanatomical landmarks.

## Results

Demographic characteristics and neuropsychological scores are shown in Table 1. No significant differences in gender, age and educational level were noted between the two experimental groups (Table 1). MMSE scores in the AD group however, were significantly lower than that in the control group using the two-sample $t$ test ($P < 0.0001$). There was not significant difference in head motion measured in peak displacement between the two groups using the two-sample $t$ test [$t(24) = 0.43$, $P = 0.68$]. Therefore, the AD patients and elderly controls in the present study were similar in head motion characteristics.

*Hippocampal connectivity analyses within the healthy age-matched group and within the AD group*

In the healthy age-matched group, the right (Fig. 2A) and left (Fig. 2B) hippocampi showed significant connectivity to a number of brain regions. Among these regions, the medial prefrontal cortex (MPFC), ventral anterior cingulate cortex (vACC), orbitofrontal cortex (OFC), posterior cingulate cortex (PCC), precuneus (PCu), left inferior temporal cortex and right inferior parietal cortex (IPC) overlap with regions underlying the default mode network (Greicuis et al., 2003). Visual inspection of the connectivity maps revealed that the magnitude and extent of right hippocampal connectivity to other brain regions, such as MPFC/vACC/OFC, PCC/PCu, bilateral temporopolar cortices, were both greater than those of the left hippocampus in the elderly control group. The right hippocampus also showed a significant connectivity to more brain regions than did the left hippocampus in the elderly control group. Right (Fig. 3A) and left (Fig. 3B) hippocampal connectivity in the AD group did not show the rightward asymmetry that was noted in the elderly control group.

*Difference in hippocampal connectivity between the healthy age-matched group and the AD group*

When comparing right hippocampal connectivity between the control and AD groups, a set of regions, including dorsal MPFC, MPFC/vACC, right cuneus extending into precuneus, left cuneus (bilateral cunei are located at the dorsal stream of the extrastriate

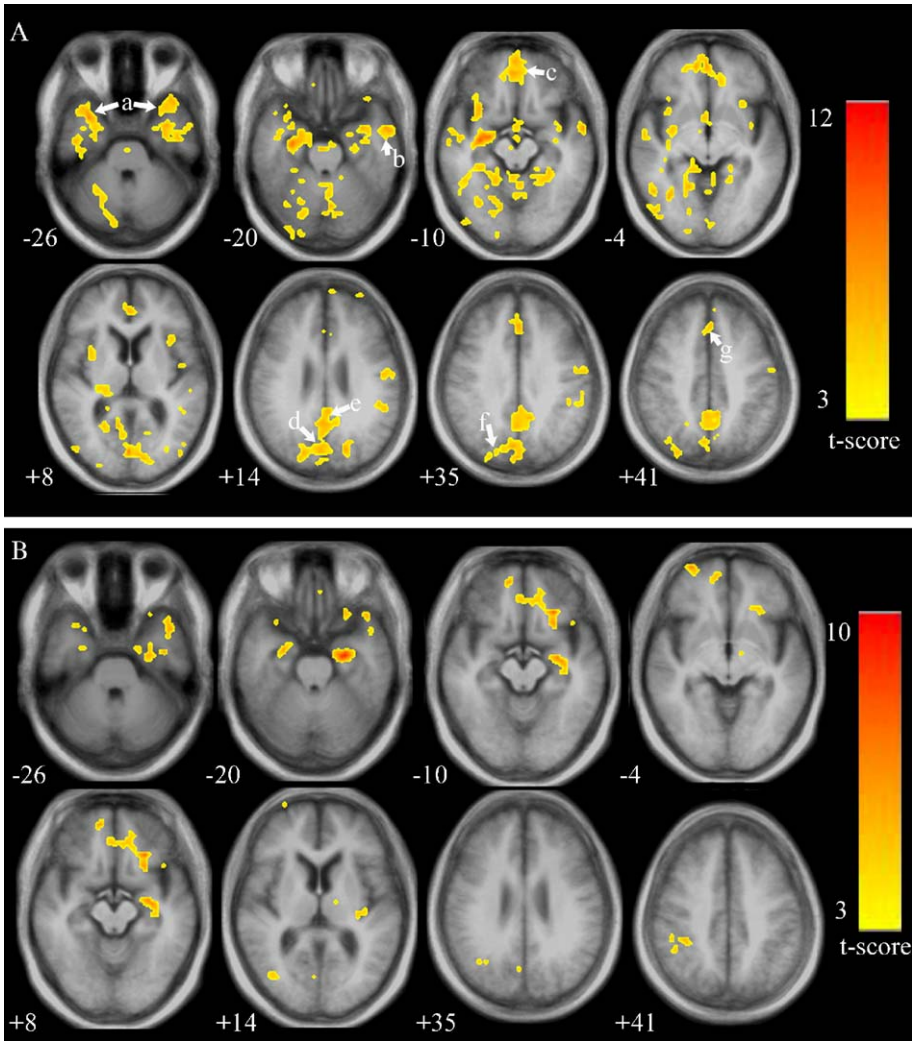


Fig. 2. Brain regions show significant connectivity to the right hippocampus (A) and left hippocampus (B) in the healthy age-matched control group. Among regions showing significant connectivity to the right hippocampus (A), MPFC, vACC, OFC, PCC, PCu, left inferior temporal cortex and right IPC overlap with the regions underlying the default mode network. a = bilateral temporopolar cortices; b = left inferior temporal cortex; c = OFC, and extend superiorly to MPFC/vACC (seen at z = −4, +8); d = Precuneus; e = PCC; f = right IPC and g = MPFC. Contrasting the right hippocampal connectivity map (A) with the left hippocampal connectivity map (B), reveals that the magnitude and extent of right hippocampal connectivity to other brain regions, such as MPFC/vACC/OFC, PCC/PCu, bilateral temporopolar cortices, are both greater than those of the left hippocampus, and that the right hippocampus shows significant connectivity to more brain regions than does the left hippocampus. The statistical map is superimposed on transverse sections of the group-average structural images. The numbers below each image refer to the z plane coordinates of Talairach and Tournoux. Left in picture is right in the brain. T score is shown on the right. Voxels with $|t(12)| \geq 3.054$ ($P < 0.01$) and cluster size $\geq 513$ mm$^3$ were taken as being significantly connected to the hippocampus. These criteria met corrected threshold of $P < 0.004$.

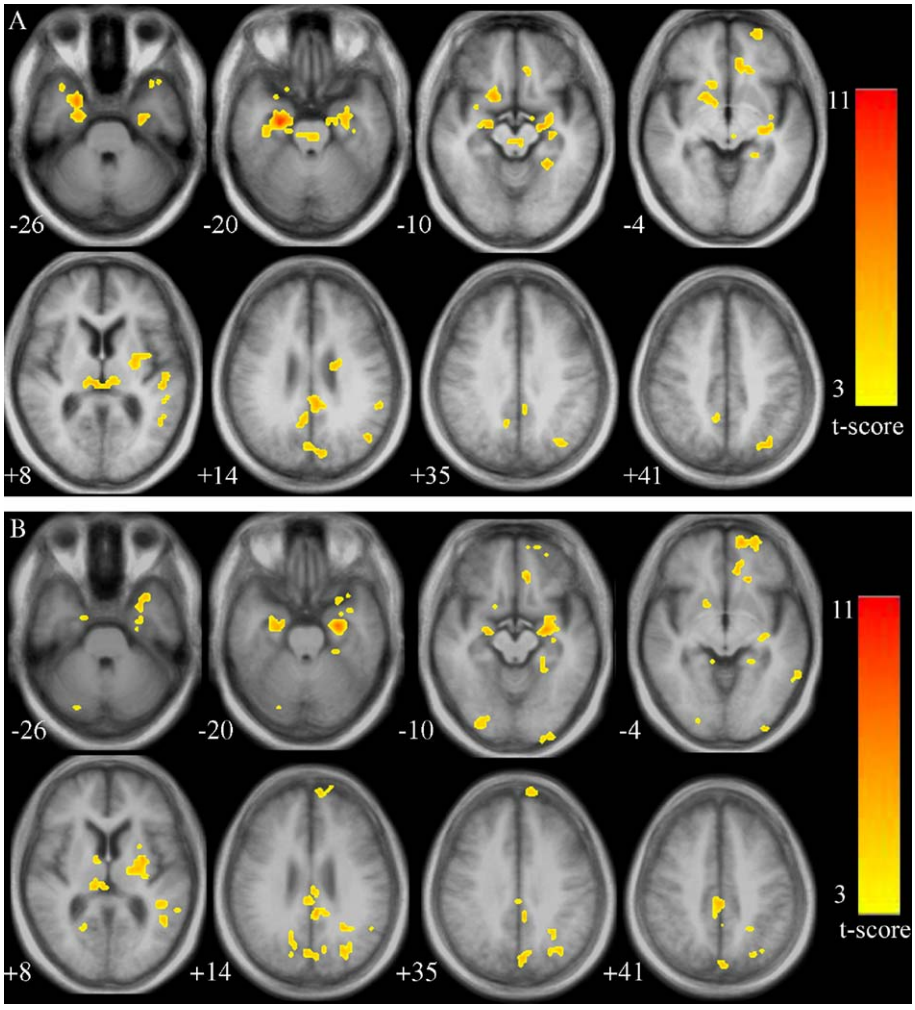


Fig. 3. Right (A) and left (B) hippocampal connectivity maps in the AD group. Visual inspection reveals that asymmetry of hippocampal connectivity present in healthy age-matched control group was diminished in AD group. Voxels with $|t(12)| \geq 3.054$ ($P < 0.01$) and cluster size $\geq 513$ mm$^3$ were taken as being significantly connected to the hippocampus. These criteria met corrected threshold of $P < 0.004$. Other details are in Fig. 2.

cortex in this study), right inferotemporal cortex (ITC) (inferotemporal cortex contains the inferior temporal gyrus (BA 20) (also called area TE) and the perirhinal cortex in this study), right superior temporal gyrus (STG) and middle temporal gyrus (MTG) (Fig. 4A), the right PCC (i.e., retrosplenial cortex in this study) (Fig. 4B), showed significantly decreased connectivity to the right hippocampus in the AD group. Specific cluster locations are shown in Table 2. Among them, the right PCC survived the height but not the extent threshold. A sagittal view obtained from a representative subject highlights the region with a 10-voxel cluster (270 mm$^3$) in the right PCC (Fig. 4B). Comparing left hippocampal connectivity between the control and AD groups, a region (peak Talairach coordinates $x$, $y$, $z$: 19 32 41; maximum $t$: −3.69) with a 20-voxel cluster (540 mm$^3$) in the right dorsolateral prefrontal cortex (DLPFC) (BA 8 and BA 9) showed a significantly increased connectivity to the left hippocampus in the AD group (Fig. 4C).

## Discussion

Two recent studies have addressed the issue of changes in LFFs in AD. Li et al. (2002) found decreased synchrony of LFFs within the hippocampus in AD. Using an independent component analysis approach to extract the network from the low frequency component of fMRI signals, Greicius et al. (2004) showed that resting-state activity in the PCC and the hippocampus is deficient in AD. The present study extended these two previous findings by investigating hippocampal connectivity, i.e., correlating the LFFs in the hippocampus with those in all other brain regions. Three main findings were generated: first, the right hippocampal connectivity to a set of regions was disrupted in AD; second, the left hippocampal connectivity to the right DLPFC was increased in AD; third, hippocampal connectivity in control subjects displayed rightward asymmetry that was diminished in AD patients.

We found that the MPFC (BA 8 and BA 10) and vACC (BA 24 and BA 32) showed disrupted connectivity to the right hippocampus (Fig. 4A). The MPFC is one of those brain regions having the highest metabolic activity at rest (Raichle et al., 2001) and exhibits "deactivation" across a variety of goal-directed behaviors (Shulman et al., 1997; Raichle et al., 2001). Moreover, the MPFC (Raichle et al., 2001; Gusnard and Raichle, 2001; Fox et al., 2005), vACC (Greicius et al., 2003) and the hippocampus (Greicius et al., 2004; Fox et al., 2005) are among those brain regions constituting the cohesive default mode network. Furthermore, there is

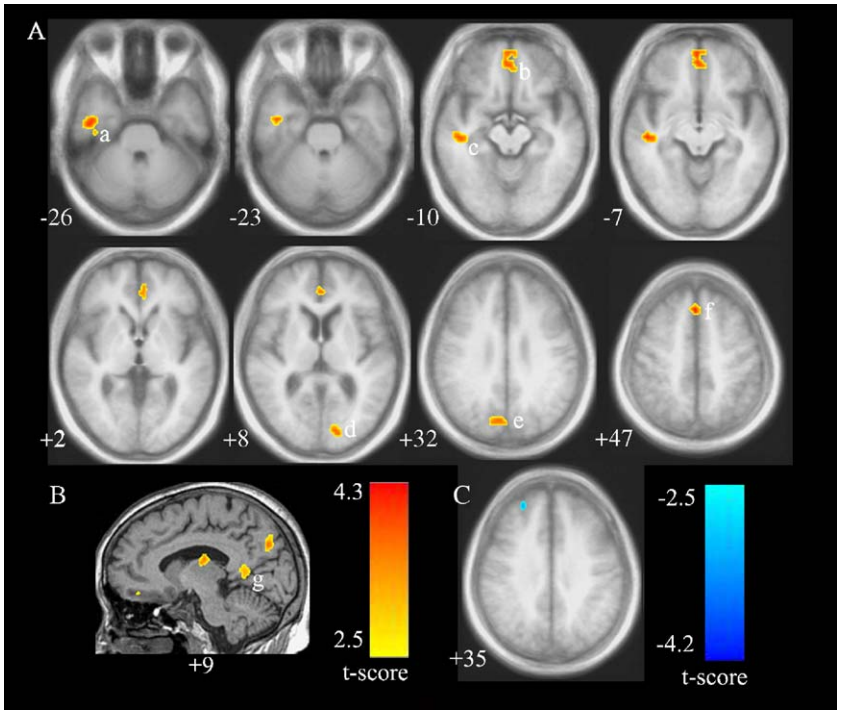


Fig. 4. Alterations in hippocampal connectivity in mild AD subjects. Regions showing decreased connectivity to the right hippocampus in AD subjects are indicated with hot color. Regions showing increased connectivity with the left hippocampus in AD subjects are indicated with cool color. (A) Regions that had decreased connectivity to the right hippocampus include dorsal MPFC, MPFC/vACC, right cuneus extending into precuneus, left cuneus, right ITC, right STG and MTG in the AD group. a = ITC (including area TE and perirhinal cortex); b = MPFC and vACC; c = STG and MTG; d = left cuneus; e = right cuneus extending into precunes, f = dorsal MPFC. (B) A sagittal view obtained from a representative subject highlights a 10-voxel cluster (270 $mm^3$) in the right PCC (i.e., the right retrosplenial cortex) that survived the height but not the extent threshold. g = PCC (i.e., the right retrosplenial cortex). (C) A region with a 20-voxel cluster (540 $mm^3$) in the right lateral prefrontal cortex (BA 9) shows significantly increased connectivity to the left hippocampus in the AD group. Voxels with $|t(24)| \geq 2.492$ ($P < 0.02$) and cluster size $\geq$513 $mm^3$ were considered to be significantly different in hippocampal connectivity between the two groups. These criteria met corrected threshold of $P < 0.05$. Other details are in Fig. 2.

substantial evidence from neuroimaging studies indicating that the MPFC and ACC are activated by episodic retrieval, especially by an autobiographical event (Cabeza, et al., 2004; Levine et al., 2004). For instance, Cabeza et al. (2004) found increased activity in a network including MPFC, ACC, bilateral visual cortices and the hippocampus during an autobiographic retrieval task. These activated regions overlap considerably with these disconnected regions we observed in this study. Combining these two facts with the current finding, the decreased hippocampal connectivity to the MPFC and the vACC may embody decreased activity of the default mode network and contribute to episodic memory impairment in AD.

The right hippocampus has shown decreased connectivity to right cuneus extending into precuneus, left cuneus and right ITC (area TE) (Fig. 4A). The right cuneus extending into precuneus and left cuneus are located at the dorsal stream of the extrastriate cortex in this study. The right ITC (area TE) is the end of the ventral visual stream (Tanaka, 1996) and is also considered to be the repository of long-term visual memory (Miyashita, 1993). Thus, we have demonstrated disrupted connectivity between the hippo-

Table 2
Regions showing disrupted connectivity to right hippocampus in AD subjects

| Brain regions | BA | Vol, $mm^3$ | Stereotaxic coordinates, mm | | | Maximum $t$ |
|---|---|---|---|---|---|---|
| | | | $x$ | $y$ | $z$ | |
| Dorsal MPFC | 8 | 513 | 2 | 25 | 47 | 4.26 |
| Left cuneus | 18/19 | 648 | −13 | −81 | 12 | 4.13 |
| MPFC/vACC | 10/24/32 | 1512 | −2 | 40 | 6 | 4.04 |
| Right MTG/STG | 21/22 | 513 | 46 | −19 | −6 | 3.98 |
| Right ITC | 35/20 | 648 | 46 | −14 | −24 | 3.84 |
| Right cuneus/PCu | 19/7 | 567 | 4 | −72 | 32 | 3.71 |
| Right PCC | 29 | 270 | 10 | −52 | 5 | 3.60[a] |

BA, Brodmann's area; $x$, $y$, $z$, coordinates of primary peak locations in the space of Talairach (Talairach and Tournoux, 1988); Vol, cluster volume; MPFC, medial prefrontal cortex; vACC, ventral anterior cingulate cortex; MTG, middle temporal gyrus; STG, superior temporal gyrus; ITC, inferotemporal cortex; PCu, precuneus; and PCC, posterior cingulate cortex.

[a] The region in right PCC survived the height but not the extent threshold. $P < 0.05$, corrected for multiple comparisons.

campus and higher-order visual cortices in early AD. It is noteworthy that the visual cortices are activated not only by visual stimuli but by visual mental imagery (Kosslyn et al., 2001). Indeed, strong evidence indicates that brain regions, which process perceptual information, are also involved in remembering and imagery, and these domain-specific cortical regions may be reactivated during remembering and contribute to the contents of a memory (Buckner and Wheeler, 2001). More importantly, previous studies have proposed that retrieval of visual information from episodic long-term memory is subserved by neural interactions between medial temporal lobe structures and posterior neocortex (Kohler et al., 1998; Buckner and Wheeler, 2001). For instance, dorsal regions (e.g., parietal–occipital sulcus) showed positive interactions with the medial temporal lobe during retrieval of information of spatial location (Kohler et al., 1998). Therefore, the functional disconnection between the hippocampus and these visual cortices in the resting-brain may reflect a breakdown of hippocampus-related cortical networks in AD.

Reduced connectivity between the hippocampus and the PCC is hypothesized to explain the decreased metabolism in the PCC in early AD (Minoshima et al., 1997). Our finding (Fig. 4B) is consistent with Greicius et al. (2004)'s study showing decreased hippocampus-PCC connectivity and is also compatible with the disconnection hypothesis.

We also found increased connectivity between the left hippocampus and the right DLPFC in AD patients (Fig. 4C). Previous studies have reported increased activity in the right DLPFC (Grady et al., 2003; Rosano et al., 2005), and increased functional connectivity within the prefrontal regions (Horwitz et al., 1995) or between the prefrontal regions and other brain regions (Grady et al., 2003) during various memory tasks in AD. This increased activity (Bookheimer et al., 2000) and connectivity (Grady et al., 2003) has been interpreted to be compensatory recruitment of cognitive resources to maintain task performance in AD patients. The increased resting-state hippocampal connectivity to the right DLPFC in our study is consistent with Grady et al. (2003)'s assumption that AD patients could use additional neural resources in prefrontal regions to compensate for losses of cognitive function.

Visual inspection of hippocampal connectivity within AD and control groups indicated that hippocampal connectivity in healthy controls present rightward asymmetry, which was diminished in AD patients (Figs. 2 and 3). Interestingly, several MRI-based measurement studies have shown the rightward asymmetry of hippocampal volume in normal adults (Szabo et al., 2001; Pedraza et al., 2004) and such anatomically rightward asymmetry was diminished in AD (Geroldi et al., 2000; Bigler et al., 2002). These findings appeared to be consistent with our observation regarding asymmetry of hippocampal connectivity. Further study on the relationship between hippocampal volume and hippocampal connectivity is needed.

Finally, there are technical and biological limitations in the present study. To study functional connectivity between the hippocampus and all other brain regions, we used a lower sampling rate for multislice acquisitions. Under such circumstance, the cardiac and respiratory fluctuation effects were aliased into the LFFs (Lowe et al., 1998; Dagli et al., 1999). These aliasing effects could reduce the specificity of the connectivity effect (Lowe et al., 1998), or even might further confound the detected differences in hippocampal connectivity between the two groups. In the future, by simultaneously recording the respiratory and cardiac cycle during the acquisition of whole-brain imaging data, these physiological effects may be estimated and removed; or focusing on some specific regions with higher sampling rate acquisition, these physiological effects may be excluded. Second, given that the resting state is associated with spontaneous thoughts and cognitive processing (Andreasen et al., 1995; Shulman et al., 1997), we cannot exclude the possibility that differences in hippocampal connectivity between the two groups, to some extent, resulted from differential spontaneous thoughts between the AD patients and elderly controls. In the future, asking the subjects to report their spontaneous thoughts after scanning is completed may contribute to exploring the between-group behavioral differences in such a resting-state fMRI study.

In summary, the current study augments the notion of decreased activity in default mode network activity in early AD and offers a clue to reduced integrity in hippocampus-related networks in early AD. In the future, we will explore correlations between the resting state hippocampal connectivity and neuropsychological data, and study whether changes in hippocampal connectivity could be a marker for cognitive decline in the early stages of AD.

## Acknowledgments

The authors would like to thank Prof. Mark J. Lowe for providing the program that we used to detect the head motion. The authors also thank Cheng Zhao, Wen Qin, Lige Gong and Zhuoxia Liu at Xuanwu Hospital Department of Radiology for their valuable assistance in performing this study. The authors gratefully acknowledge Dr. Rhoda Perozzi for editing and proofreading assistance. This study was partially supported by Foundation of Beijing Brain Aging Key Laboratory, Grant No. 951890600, the Natural Science Foundation of China, Grant Nos. 30425004 and 60121302, and the National Key Basic Research and Development Program (973) Grant No. 2004CB318107.

## References

American Psychiatric Association, 1994. DSM-IV: Diagnostic and Statistical Manual of Mental Disorders, 4th ed. Am. Psychiatric Assoc. Press, Washington, DC.

Andreasen, N.C., O'Leary, D.S., Cizadlo, T., Arndt, S., Rezai, K., Watkins, G.L., Ponto, L.L., Hichwa, R.D., 1995. Remembering the past: two facets of episodic memory explored with positron emission tomography. Am. J. Psychiatry 152, 1576–1585.

Bigler, E.D., Tate, D.F., Millerm, M.J., Rice, S.A., Hessel, C.D., Earl, H.D., Tschanz, J.T., Plassman, B., Welsh-Bohmer, K.A., 2002. Dementia, asymmetry of temporal lobe structures, and apolipoprotein E genotype: relationships to cerebral atrophy and neuropsychological impairment. J. Int. Neuropsychol. Soc. 8, 925–933.

Biswal, B., Yetkin, F.Z., Haughton, V.M., Hyde, J.S., 1995. Functional connectivity in the motor cortex of resting human brain using echo-planar MRI. Magn. Reson. Med. 34, 537–541.

Biswal, B.B., Van Kylen, J., Hyde, J.S., 1997a. Simultaneous assessment of flow and BOLD signals in resting-state functional connectivity maps. NMR Biomed. 10, 165–170.

Biswal, B., Hudetz, A.G., Yetkin, F.Z., Haughton, V.M., Hyde, J.S., 1997b. Hypercapnia reversibly suppresses low-frequency fluctuations in the human motor cortex during rest using echo-planar MRI. J. Cereb. Blood Flow Metab. 17, 301–308.

Bookheimer, S.Y., Strojwas, M.H., Cohen, M.S., Saunders, A.M., Pericak-Vance, M.A., Mazziotta, J.C., Small, G.W., 2000. Patterns of brain

activation in people at risk for Alzheimer's disease. N. Engl. J. Med. 343, 450–456.
Buckner, R.L., Wheeler, M.E., 2001. The cognitive neuroscience of remembering. Nat. Rev., Neurosci. 2, 624–634.
Cabeza, R., Prince, S.E., Daselaar, S.M., Greenberg, D.L., Budde, M., Dolcos, F., LaBar, K.S., Rubin, D.C., 2004. Brain activity during episodic retrieval of autobiographical and laboratory events: an fMRI study using a novel photo paradigm. J. Cogn. Neurosci. 16, 1583–1594.
Cordes, D., Haughton, V.M., Arfanakis, K., Carew, J.D., Turski, P.A., Moritz, C.H., Quigley, M.A., Meyerand, M.E., 2001. Frequencies contributing to functional connectivity in the cerebral cortex in "resting-state" data. AJNR Am. J. Neuroradiol. 22, 1326–1333.
Cox, R.W., 1996. AFNI: software for analysis and visualization of functional magnetic resonance neuroimages. Comput. Biomed. Res. 29, 162–173.
Dagli, M.S., Ingeholm, J.E., Haxby, J.V., 1999. Localization of cardiac-induced signal change in fMRI. NeuroImage 9, 407–415.
de Lacoste, M.C., White III, C.L., 1993. The role of cortical connectivity in Alzheimer's disease pathogenesis: a review and model system. Neurobiol. Aging 14, 1–16.
Delbeuck, X., Van der Linden, M., Collette, F., 2003. Alzheimer's disease as a disconnection syndrome? Neuropsychol. Rev. 13, 79–92.
Duvernoy, H.M., 1998. Structure, function, and connections. In: Duvernoy, H.M. (Ed.), The Human Hippocampus, 2nd ed. Springer-Verlag Press, Berlin Heidelberg, pp. 26–38.
Fox, M.D., Snyder, A.Z., Vincent, J.L., Corbetta, M., Van Essen, D.C., Raichle, M.E., 2005. The human brain is intrinsically organized into dynamic, anticorrelated functional networks. Proc. Natl. Acad. Sci. U. S. A. 102, 9673–9678.
Friston, K.J., Frith, C.D., Liddle, P.F., Frackowiak, R.S., 1993. Functional connectivity: the principal-component analysis of large (PET) data sets. J. Cereb. Blood Flow Metab. 13, 5–14.
Geroldi, C., Laakso, M.P., DeCarli, C., Beltramello, A., Bianchetti, A., Soininen, H., Trabucchi, M., Frisoni, G.B., 2000. Apolipoprotein E genotype and hippocampal asymmetry in Alzheimer's disease: a volumetric MRI study. J. Neurol., Neurosurg. Psychiatry 68, 93–96.
Grady, C.L., Furey, M.L., Pietrini, P., Horwitz, B., Rapoport, S.I., 2001. Altered brain functional connectivity and impaired short-term memory in Alzheimer's disease. Brain 124, 739–756.
Grady, C.L., McIntosh, A.R., Beig, S., Keightley, M.L., Burian, H., Black, S.E., 2003. Evidence from functional neuroimaging of a compensatory prefrontal network in Alzheimer's disease. J. Neurosci. 23, 986–993.
Greicius, M.D., Krasnow, B., Reiss, A.L., Menon, V., 2003. Functional connectivity in the resting brain: a network analysis of the default mode hypothesis. Proc. Natl. Acad. Sci. U. S. A. 100, 253–258.
Greicius, M.D., Srivastava, G., Reiss, A.L., Menon, V., 2004. Default-mode network activity distinguishes Alzheimer's disease from healthy aging: evidence from functional MRI. Proc. Natl. Acad. Sci. U. S. A. 101, 4637–4642.
Gusnard, D.A., Raichle, M.E., 2001. Searching for a baseline: functional imaging and the resting human brain. Nat. Rev., Neurosci. 2, 685–694.
Hampson, M., Peterson, B.S., Skudlarski, P., Gatenby, J.C., Gore, J.C., 2002. Detection of functional connectivity using temporal correlations in MR images. Hum. Brain Mapp. 15, 247–262.
Hirano, A., Zimmerman, H.M., 1962. Alzheimer's neurofibrillary changes—A topographic study. Arch. Neurol. 7, 227–242.
Holmes, A.P., Friston, K.J., 1998. Generalisability, random effects and population inference. NeuroImage 7, S754.
Horwitz, B., McIntosh, A.R., Haxby, J.V., Furey, M., Salerno, J.A., Schapiro, M.B., Rapoport, S.I., Grady, C.L., 1995. Network analysis of PET-mapped visual pathways in Alzheimer type dementia. NeuroReport 27, 2287–2292.
Hyman, B.T., Van Horsen, G.W., Damasio, A.R., Barnes, C.L., 1984. Alzheimer's disease: cell-specific pathology isolates the hippocampal formation. Science 225, 1168–1170.
Hyman, B.T., Van Hoesen, G.W., Kromer, L.J., Damasio, A.R., 1986. Perforant pathway changes and the memory impairment of Alzheimer's disease. Ann. Neurol. 20, 472–481.
Jiang, A., Kennedy, D.N., Baker, J.R., Weisskoff, R.M., Tootell, R.B., Woods, R.P., Benson, R.R., Kwong, K.K., Brady, T.J., Rosen, B.R., Belliveau, J.W., 1995. Motion detection and correction in functional MR imaging. Hum. Brain Mapp. 3, 224–235.
Jiang, T., He, Y., Zang, Y., Weng, X., 2004. Modulation of functional connectivity during the resting state and the motor task. Hum. Brain Mapp. 22, 63–71.
Kohler, S., McIntosh, A.R., Moscovitch, M., Winocur, G., 1998. Functional interactions between the medial temporal lobes and posterior neocortex related to episodic memory retrieval. Cereb. Cortex 8, 451–461.
Kosslyn, S.M., Ganis, G., Thompson, W.L., 2001. Neural foundations of imagery. Nat. Rev., Neurosci. 2, 635–642.
Levine, B., Turner, G.R., Tisserand, D., Hevenor, S.J., Graham, S.J., McIntosh, A.R., 2004. The functional neuroanatomy of episodic and semantic autobiographical remembering: a prospective functional MRI study. J. Cogn. Neurosci. 16, 1633–1646.
Li, S.J., Li, Z., Wu, G., Zhang, M.J., Franczak, M., Antuono, P.G., 2002. Alzheimer Disease: evaluation of a functional MR imaging index as a marker. Radiology 225, 253–259.
Lowe, M.J., Mock, B.J., Sorenson, J.A., 1998. Functional connectivity in single and multislice echoplanar imaging using resting-state fluctuations. NeuroImage 7, 119–132.
Lowe, M.J., Dzemidzic, M., Lurito, J.T., Mathews, V.P., Phillips, M.D., 2000. Correlations in low-frequency BOLD fluctuations reflect cortico-cortical connections. NeuroImage 12, 582–587.
McKhann, G., Drachman, D., Folstein, M., Price, D., Stadlan, E.M., 1984. Clinical diagnosis of Alzheimer's disease: report of the NINCDS-ADRDA Work Group under the auspices of the department of Health and Human Services Task Force on Alzheimer's disease. Neurology 34, 939–944.
Minoshima, S., Giordani, B., Berent, S., Frey, K.A., Foster, N.L., Kuhl, D.E., 1997. Metabolic reduction in the posterior cingulate cortex in very early Alzheimer's disease. Ann. Neurol. 42, 85–94.
Miyashita, Y., 1993. Inferior temporal cortex: where visual perception meets memory. Annu. Rev. Neurosci. 16, 245–263.
Morris, J.C., 1993. The Clinical Dementia Rating (CDR): current version and scoring rules. Neurology 43, 2412–2414.
Morris, J.C., Storandt, M., Miller, J.P., McKeel, D.W., Price, J.L., Rubin, E.H., Berg, L., 2001. Mild cognitive impairment represents early-stage Alzheimer disease. Arch. Neurol. 58, 397–405.
Nestor, P.J., Scheltens, P., Hodges, J.R., 2004. Adance in the early detection of Alzheimer's disease. Nat. Rev., Neurosci. 5, s34–s41.
Pedraza, O., Bowers, D., Gilmore, R., 2004. Asymmetry of the hippocampus and amygdala in MRI volumetric measurements of normal adults. J. Int. Neuropsychol. Soc. 10, 664–678.
Press, W.H., Teukolsky, S.A., Vetterling, W.T., Flannery, B.P., 1992. Numerical Recipes in C, 2nd ed. U.K. Cambridge Univ. Press, Cambridge.
Raichle, M.E., MacLeod, A.M., Snyde, rA.Z., Powers, W.J., Gusnard, D.A., Shulman, G.L., 2001. A default mode of brain function. Proc. Natl. Acad. Sci. U. S. A. 98, 676–682.
Rombouts, S.A., Stam, C.J., Kuijer, J.P., Scheltens, P., Barkhof, F., 2003. Identifying confounds to increase specificity during a "no task condition". Evidence for hippocampal connectivity using fMRI. NeuroImage 20, 1236–1245.
Rosano, C., Aizenstein, H.J., Cochran, J.L., Saxton, J.A., De Kosky, S.T., Newman, A.B., Kuller, L.H., Lopez, O.L., Carter, C.S., 2005. Event-related functional magnetic resonance imaging investigation of executive control in very old individuals with mild cognitive impairment. Biol. Psychiatry 57, 761–767.
Shulman, G.L., Fiez, J.A., Corbetta, M., Buckner, R.L., Miezin, F.M., Raichle, M.E., Petersen, S.E., 1997. Common blood flow changes across visual tasks: decrease in cerebral cortex. J. Cogn. Neurosci. 9, 648–663.
Sperling, R., Chua, E., Cocchiarella, A., Rand-Giovannetti, E., Poldrack,

R., Schacter, D.L., Albert, M., 2003. Putting names to faces: successful encoding of associative memories activates the anterior hippocampal formation. NeuroImage 20, 1400–1410.

Stein, T., Moritz, C., Quigley, M., Cordes, D., Haughton, V., Meyerand, E., 2000. Functional connectivity in the thalamus and hippocampus studied with functional MR imaging. AJNR Am. J. Neuroradiol. 21, 1397–1401.

Szabo, C.A., Xiong, J., Lancaster, J.L., Rainey, L., Fox, P., 2001. Amygdalar and hippocampal volumetry in control participants: differences regarding handedness. AJNR Am. J. Neuroradiol. 22, 1342–1345.

Talairach, J., Tournoux, P., 1988. Co-Planar Stereotaxic Atlas of the Human Brain. Thieme Verlag, Stuttgart.

Tanaka, K., 1996. Inferotemporal cortex and object vision. Annu. Rev. Neurosci. 19, 109–139.

Terry, R.D., 1991. Physical basis of cognitive alteration in Alzheimer's disease: synapse loss is the major correlate of cognitive impairment. Ann. Neurol. 30, 572–580.

Watson, C., Andermann, F., Gloor, P., Jones-Gotman, M., Peters, T., Evans, A., Olivier, A., Melanson, D., Leroux, G., 1992. Anatomic basis of amygdaloid and hippocampal volume measurement by magnetic resonance imaging. Neurology 42, 1743–1750.